

Design and Analysis of Gas Insulated Busduct with Polymeric Spacers under Void Defect

A. Jagadeesh, G.V. Sivakrishna Rao and G.V. Nagesh Kumar

Abstract: Due to rapid growth of population, energy utilization increased which substantial required reliable, economical and flexible technology to meet the demand. The unique properties of Gas insulated systems (GIS) made it an alternative to meet the demand. Power engineers face a lot of challenges during GIS components design. GIS generally fail to operate in case of insulation and spacer failures as it leads to increase of electric field stress at the triple junction. Though utmost care has been taken during the manufacturing process, minute imperfections in the form of voids, delimitations, protrusions, cracks, etc., can occur which leads to the operation failure of GIS. Hence, for high level of dependability, vital importance is to be given to the electric field pattern along the surface periphery of the spacer. In this paper, analysis of electric field for a Polymeric spacer with different Filler concentrations of Nitrates, Carbides and Oxides under the void imperfection is carried. The reduction of Electric Field is carried with the insertion of metal inserts. The results are presented and analysed for different voltages without and with metal inserts.

Index Terms: Electric Field, Spacer, Protrusion, Gas Insulated Bus duct.

I. INTRODUCTION

Increase in energy consumption demands Gas Insulated systems. To support the stressed conductors in the system, the use of solid insulators is essential. The solid insulating spacer is noted to be the weakest point in GIS systems as it is responsible for surface flashover and breakdown in dielectric strength. Hence, there is a need for manufacturing reliable and flashover free spacers [1-3]. High field stresses results in flashover at critical level of three junctions in a spacer which in turn causes instigation of partial discharges. Spacer's profile is assumed to be the main variable responsible for field pattern and show the uniformity is attained by excepting the proper profile. [2, 6-8].

GIS distinctive features enable us to consider it above air insulated substations. During its operation, several defects like protrusions, depressions, delamination, voids, etc., occur. Hence, these improper manufacturing defects and roughness on spacer's surface affects the breakdown strength of GIS.

Insulation and spacer failures are few important aspects

that are to be taken care during the manufacturing and operation process of GIS as its failure may lead to breakdown of dielectric strength which was identified by Cookson et al. [11]. Tsuboi and Misaki [12] designed a cone type spacer and improved the surface shape of the spacer with a slight change in contact position which proved prolific in decline of local field intensification. Voids, delamination, cracks, protrusions, etc on the surface of the spacers were noticed in GIB which influenced pattern of field resulting in spacer failure of the spacer.

In this paper, Polymeric spacer has been designed and different filler concentrations of nitrates, oxides and carbides have been considered. Metallic inserts help in decreasing the field stress at triple junction. To study the affect of metal inserts, analysis without and with metal inserts have been carried under void imperfection by considering various applied voltages.

II. ELECTRIC FIELD COMPUTATION

In GIB, spacers and SF₆ gas are the two main insulating media with insulating materials as alumina and silica filled epoxy. Charge simulation method has provided acceptable results for computing electric field but was time consuming in selecting the correct count and kind of charges which resulted in the rise of FEM technology. This technique reduces the energy by segregating the region under consideration into triangular elements for 2Dimensional problems or tetrahedrons for 3Dimensional problems. The stored energy W in the portion having volume U in anisotropic dielectric material under steady state conditions by assuming Rectangular coordinate system and Laplacian field is considered as:

$$W = \frac{1}{2} \int_u \epsilon |\text{grad}V|^2 du \quad (1)$$

$$W = \frac{1}{2} \iiint_U \left[\epsilon_x \left(\frac{\partial V}{\partial x} \right)^2 + \epsilon_y \left(\frac{\partial V}{\partial y} \right)^2 + \epsilon_z \left(\frac{\partial V}{\partial z} \right)^2 \right] dx dy dz \quad (2)$$

Moreover, when minute level field behavior is considered, in two dimensional, the total energy can be determined using equation (3).

$$\frac{W}{\phi} = \frac{1}{2} * \epsilon \iint \left[\left(\frac{\partial V}{\partial x} \right)^2 + \left(\frac{\partial V}{\partial y} \right)^2 \right] dx dy \quad (3)$$

Where energy density per elementary area dA is (W/φ).

To apply minimisation criteria on the above equations, few below given assumptions are to be considered.

- V(x,y,z) is voltage distribution endless over the region and
- Its derivative may exist.

Manuscript published on 30 June 2019.

* Correspondence Author (s)

A. Jagadeesh*, Department of EEE, GITAM University, Visakhapatnam, Andhra Pradesh, INDIA.

G.V.Nagesh Kumar, Department of EEE, JNTUA College of Engineering, Pulivendula, Andhra Pradesh, INDIA.

G.V.Sivakrishna Rao, Department of EEE, Andhra University, Visakhapatnam, Andhra Pradesh, INDIA.

© The Authors. Published by Blue Eyes Intelligence Engineering and Sciences Publication (BEIESP). This is an open access article under the CC-BY-NC-ND license <http://creativecommons.org/licenses/by-nc-nd/4.0/>.

Discretization must be made to find a solution for the continuous function. Hence, considered area is subdivided into triangular elements. Thus:

$$\frac{W}{\phi} = \frac{1}{2} * \epsilon * \sum_{i=1}^n \left[\left(\frac{\partial V_x}{\partial x} \right)^2 + \left(\frac{\partial V_y}{\partial y} \right)^2 \right] * A_i \quad (4)$$

Where,

n is the total quantity of elements,

A_i corresponds to i^{th} element.

Hence minimisation of the energy within the complete system can be written as

$$\frac{\partial X}{\partial [V(x,y)]} = 0; \text{ where } X = \frac{W}{\phi} \quad (5)$$

To calculate the unknown potential at nodes, the above approximation may be taken. In Individual element the field is taken to be constant and can be determined by the following equation.

$$E = -i \frac{\partial V(x,y)}{\partial x} - j \frac{\partial V(x,y)}{\partial y} \quad (6)$$

III. POLYMERIC SPACER

In GIS, insulation clearance between high and low voltage electrodes is an important factor. Hence solid insulators are important as mechanical supports to create the insulation clearance. In the insulation of a gas-solid interface, various factors to be taken into consideration are contamination particles, voids, E- field intensification at triple junction and charging on the spacer surface along with the electric field distribution on the spacer surface. Hence, different techniques were introduced as a solution to the above considered factors.

Designing of insulating spacers was one important aspect to the electrical engineer and so they required keen knowledge on electric field distribution. Epoxy or cast resin finds great application in high voltage systems as insulation. Currently epoxy with nano reinforcement has drawn lot of interest as it improves the properties of epoxy considerably. For analysis a polymer spacer has been designed and different fillers of nitrates, carbides and oxides have been considered. The relative permittivity's, break down voltages and electric field distributions are determined and analyzed for the designed cone type spacer with different dielectric coatings of nano nitrides. Among different techniques Finite Element Method technique has been employed to compute the electric field.

For its excellent mechanical, electrical properties and chemical stability, epoxy resin is most preferred material for high voltage systems as it has high insulation because of adequate mechanical, electrical qualities as well as chemical stability. Such resins are relatively immune to chemical corrosion and work as effective generally stable to chemical attacks and are excellent adherents with slow shrinkage during curing and no volatile gas emissions. However, these advantages make epoxy use quite expensive. They can also not be expected to exceed a 140°C temperature. Their use is therefore excluded in high-tech areas where service temperatures are higher.

Polymer composite contains as its main constituents 1) polymer matrix, 2) fillers and 3) interaction zone. Nano composites of epoxy are available in dimensions below 100

nm with less percentage by weight of the total material. Such composites have good thermal conductivity, strong resistivity for temperature and high breakdown [17]. Fillers are of one dimensional or three-dimensional and have very good engineering properties including thermal, mechanical and electrical types.

In high voltage apparatus, epoxy resin is extensively in use as insulation. A practical epoxy resin has dielectric permittivity depending on the filler type. Epoxies are expensive and cannot be expected beyond a temperature of 140°C. NMC (Nano / micro composites) is useful in grading of GIS spacer by lower ϵ_1 due to reduction in loading normally less than 10 wt percent, due to their lower r . Lewis was inspired in electrical insulation by polymer nano-dielectrics as nano-dielectric insulation performs better in certain areas compared to conventional materials of insulation.

The zone of interaction for the nano-particles and the polymer matrix is considered as an independent region. If nano particles are in remote distribution, Carriers are controlled in an interaction zone which diminishes the mobility and density of carriers. Mobility of charge carriers is higher with the loading of the filler [17-19]. The strength between nano-particles and polymeric matrix has a direct influence on the thickness of the interaction zone. Nano-dielectrics shows some uniqueness caused by the large interaction zone. A structural change is seen when nano-fillers are introduced into the polymer matrix because of the interaction between polymer and nano-filler. The use of inorganic fillers such as boron nitride, aluminium nitride in polymeric matrices reduces costs, improves fire resistances and mechanical properties like tensile strength. It also increases the permittivity of epoxy nanocomposite [16, 20].

IV. CALCULATION OF RELATIVE PERMITTIVITY

The magnitude of electric field is affected by dielectric constant that is with a high dielectric constant, the electric field reduces. Nano and micro composites on combining with epoxy resin increases the overall permittivity of the composite in comparison with simple epoxy and composite epoxy. Hence, GIS preferred them.

Conductivity increases when the filler concentration is abruptly increased. The overlapping of nano and micro particles are dependable on the rate of dispersion in the epoxy resin. Lichtenecker-Rother mixing rule can be extended for the dielectric property of 2 phase dielectric materials as shown in the below equation (7)

$$\text{Log} \epsilon_c = x \text{Log} \epsilon_1 + y \text{Log} \epsilon_2 + z \text{Log} \epsilon_3 \quad (7)$$

Where ϵ_c is the final joint permittivity, $\epsilon_1, \epsilon_2, \epsilon_3$ are the permittivity of the filler and epoxy x, y, z are related to the

quantity of the filler material and polymer concentrations. The permittivity values of epoxy and that of alumina permittivity (Al₂O₃) is 3.6 and 9.2 and then the effective permittivity of 5 percent by weight of nano and 65wt percent by weight of micro is 16.759.



V. RESULTS AND DISCUSSION

Considering different filler concentrations, the electric field stress for different values of permittivity are analyzed and the results are plotted. The analysis has been done with and without metal inserts in the polymer spacers. Figure 2 represents electric potential under the presence of void with and without metal insert in the polymer spacer. Figure 3 represents the electric field stress for 72.5, 145 and 220KV applied voltages when silica nitrate filler is considered. The analysis has been done for the spacer with and without metal inserts. From the figure, it is obvious that as the filler quantity is increasing the final value of permittivity increases. Contrarily, the field stress is sufficiently less by using metal inserts. Fig.4 represents the electric field stress for Aluminum Nitrate filler for different values of voltages and it is seen that the ultimate permittivity proportional increases with filler concentration and that the electrical field stress decreases with the use of metal inserts. It can also be seen that the permittivity value for aluminum nitrate is more when compared with silica nitrate filler concentration. Table1 represents nitrate filler concentrations in a polymer spacer. As seen in the table, as and when the voltage level increases for different filler concentration values, the field at inside and outside ends also increases for a plain polymer, without and with metal inserts. It can also be noted that when the filler concentration increases, resultant permittivity value increases whereas the electric field at the inside and outside. Moreover, we can come to a conclusion that the electric field almost reduces to zero when the metal inserts have been included in the polymer spacers with the increase in applied voltage. The use of Aluminum nitrate filler concentration reduces the value of electric field stress to a great extent when compared with Silicon nitrate filler. The electric field stress for Titanium dioxide and Magnesium oxide for different values of voltages is analyzed and the resultant graphs have been represented in sfigures 5 and 6. In figs.5 and 6, It can be seen that the subsequent permittivity is higher for the higher quantity of filler and is higher in the case of titanium dioxide.

It is clearly shown that the electric field stress has been reduced to almost zero when metal inserts have been included in both the cases. In Table 2, for the concentration of oxides filler, we can observe that with the increase in applied voltage, the electric field value also increases and as the quantity of the filler increases, the resultant permittivity becomes high. The electrical field stress reduces to a high level when compared without metal inserts with the use of metal inserts. Figures 7 and 8 represent the electric field stress for Boron carbide and Silicon carbide filler material. It is noticed that the resultant permittivity value increases with the increase in filler concentration and also it can be seen that for Boron carbide the value of permittivity is more compared to silicon carbide. Also, the value of electric field stress is lessened to a greater extent when the metal inserts have been included in the spacer which can be clearly seen in table3 that represents carbide filler concentration. Hence, it can be concluded that using different filler materials and with the presence of metal insert in the polymer spacer, there is an overall reduction of electric field stress i.e. almost to zero when compared with the absence of metal inserts.

VI. CONCLUSION

The design and optimization process is of great importance for a Gas insulated Busduct. An electrical engineer can design a reliable and effective GIS if a thorough study is made on electric field distribution which in turn helps to avoid possible flashovers especially on the spacer surface and at the triple junction. Spacer’s shape plays a significant role in designing. A polymer spacer was designed and different filler concentration of nitrates, carbides, oxides have been taken for analysis. It can be observed that the resultant dielectric quality of the composite increases with the increase in filler concentration due to the addition of mixtures of nitrates, carbides and oxides to the base epoxy resin. From the tables, it can be concluded that metal inserts help in reducing the field stress. As the v applied, it can be concluded

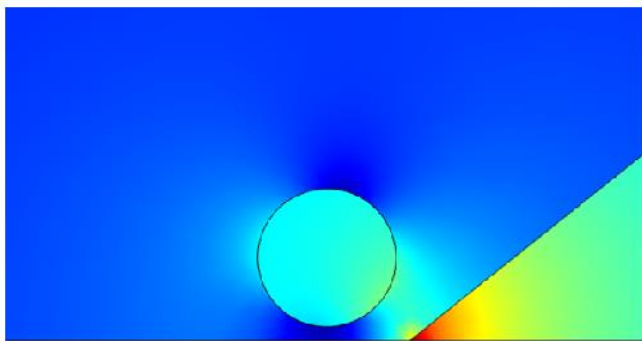


Fig. (a) Without metal inserts

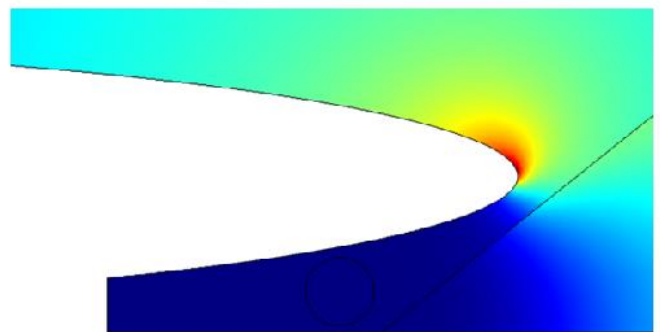


Fig. (b) With metal inserts

Fig 2 Electric potential under void

Design and Analysis of Gas Insulated Busduct with Polymeric Spacers under Void defect

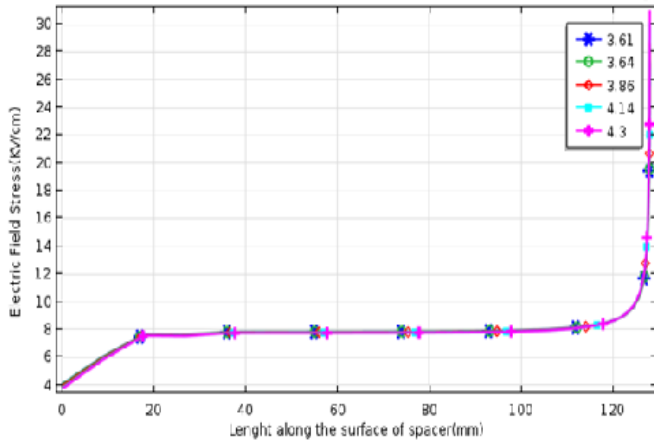


Fig. (a) Without metal inserts

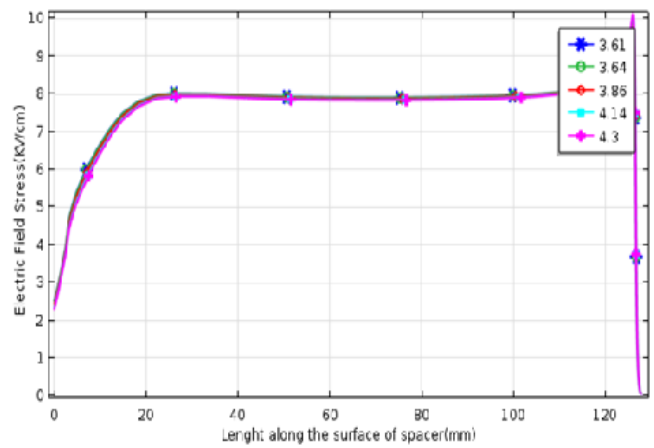


Fig. (b) With metal inserts

(i) At 72.5KV voltage

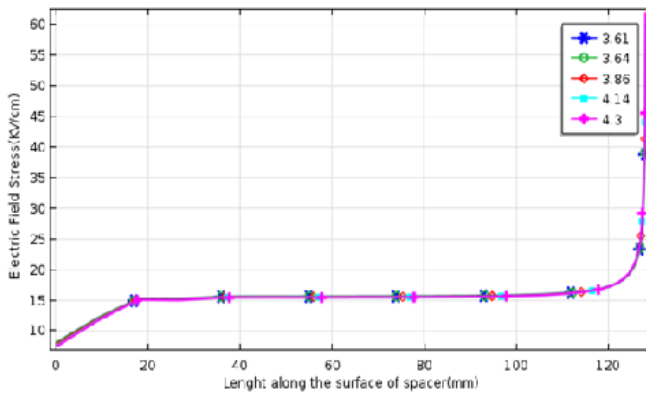


Fig. (a) without metal inserts

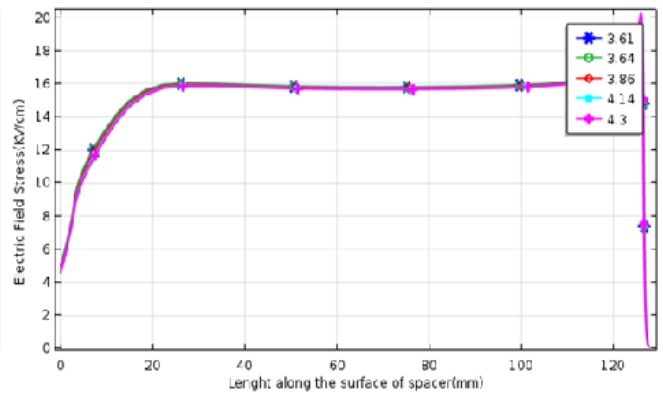


Fig. (b) With metal inserts

(ii) At 145KV voltage

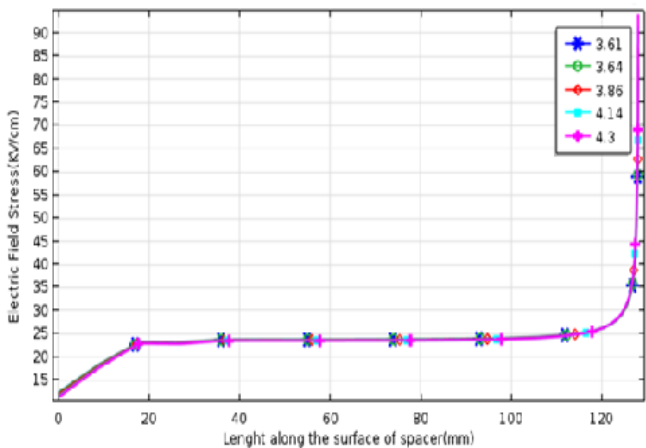


Fig. (a) Without metal inserts

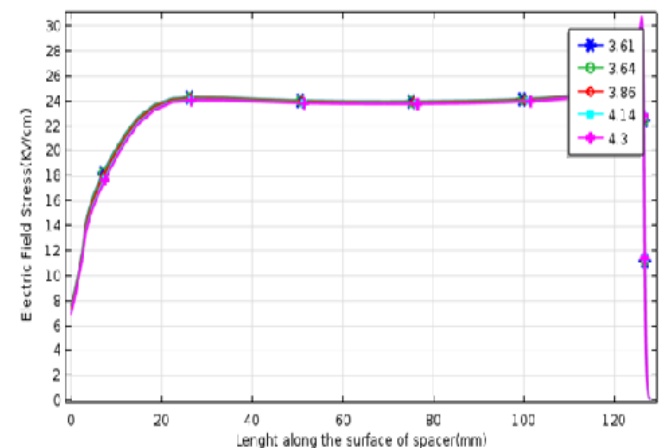


Fig.(b) With metal inserts

(iii) At 220KV voltage

Fig.3 Electric field stress with metal inserts under void for Silica Nitrates filler

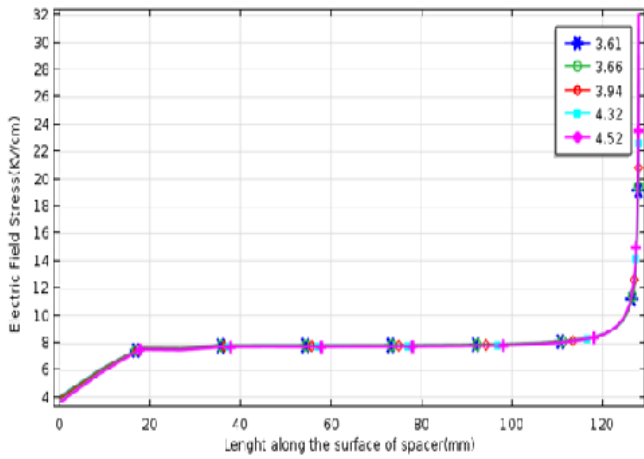


Fig. (a) Without metal inserts

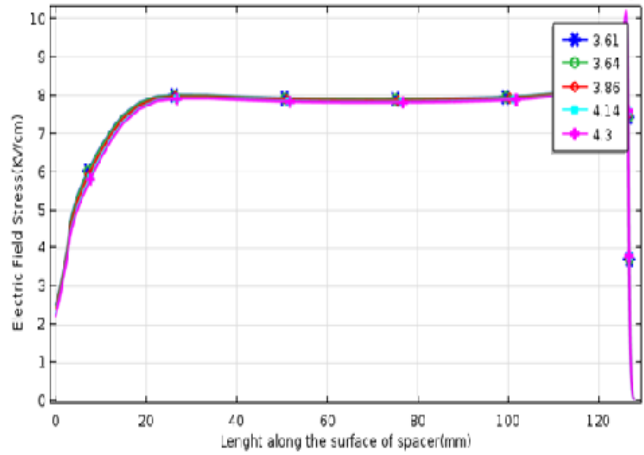


Fig. (b) With metal inserts

(i) At 72.5KV voltage

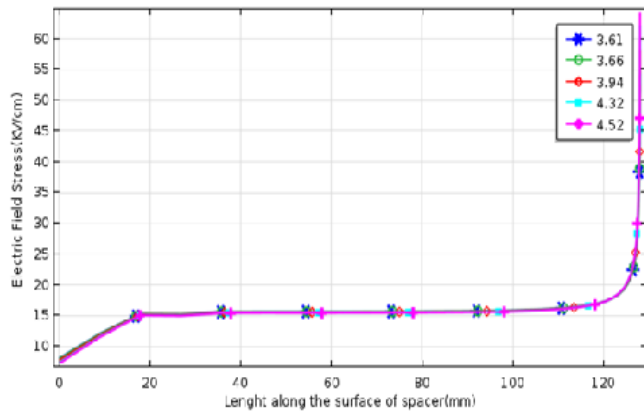


Fig. (a) Without metal inserts

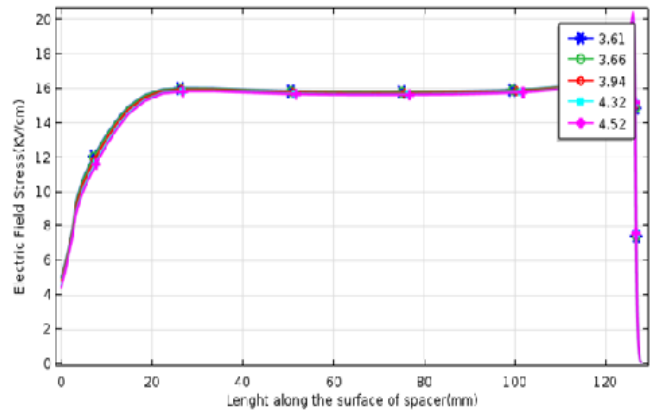


Fig. (b) With metal inserts

(ii) At 145KV voltage

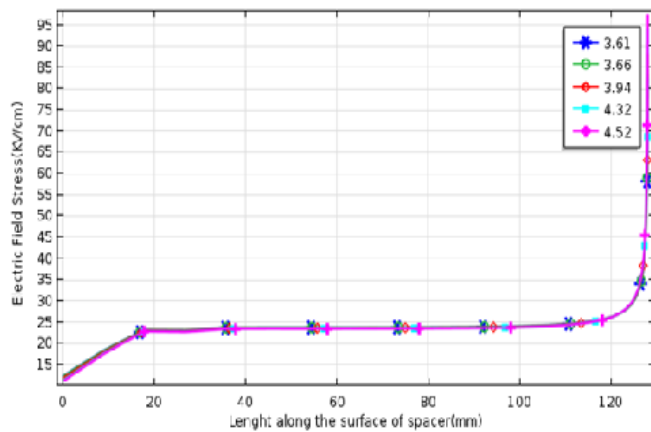


Fig. (a) Without metal inserts

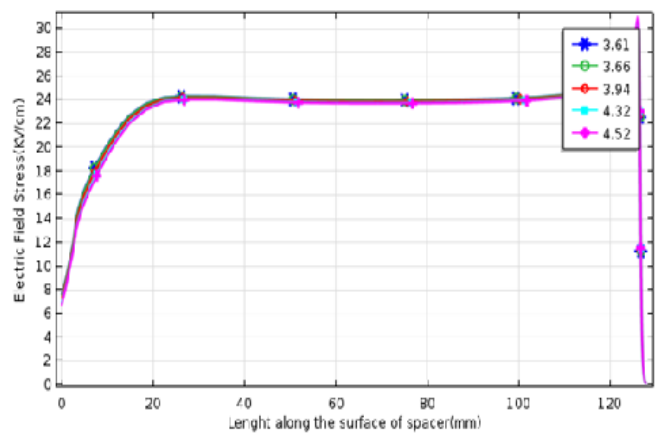


Fig. (b) With metal inserts

(iii) At 220KV voltage

Fig.4 Electric field stress with metal inserts under void for Aluminium Nitrate filler

Design and Analysis of Gas Insulated Busduct with Polymeric Spacers under Void defect

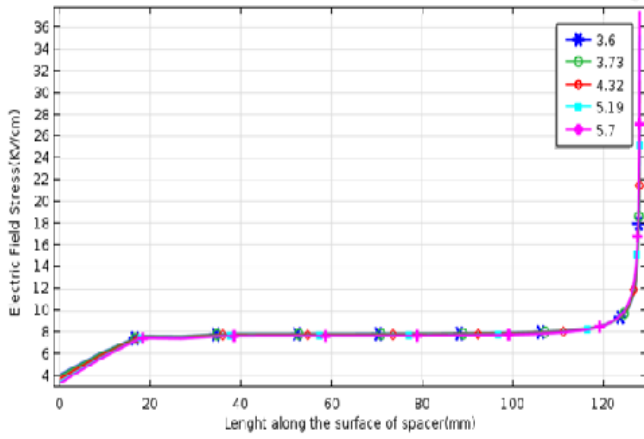


Fig. (a) Without metal inserts

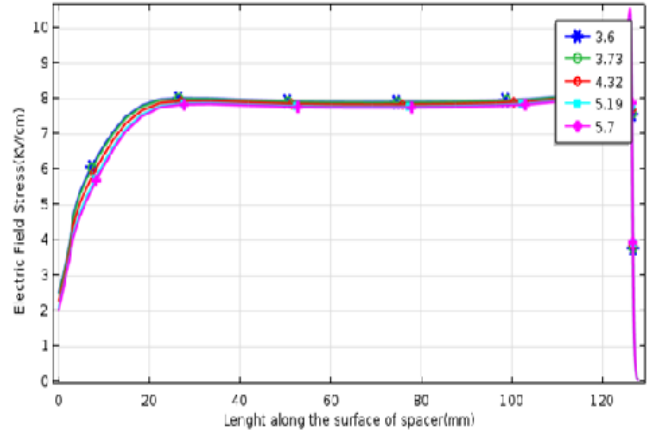


Fig. (b) With metal inserts

(i) At 72.5KV voltage

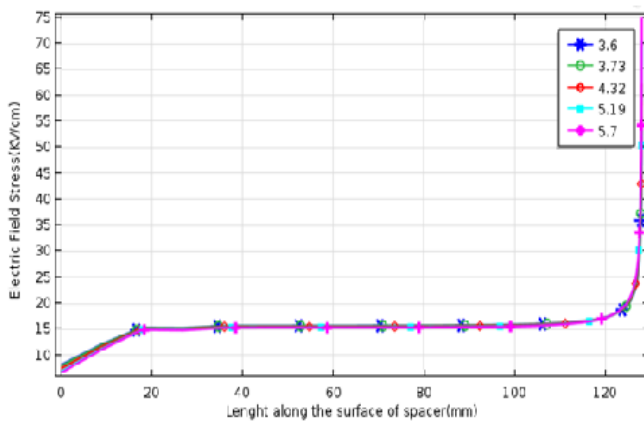


Fig. (a) Without metal inserts

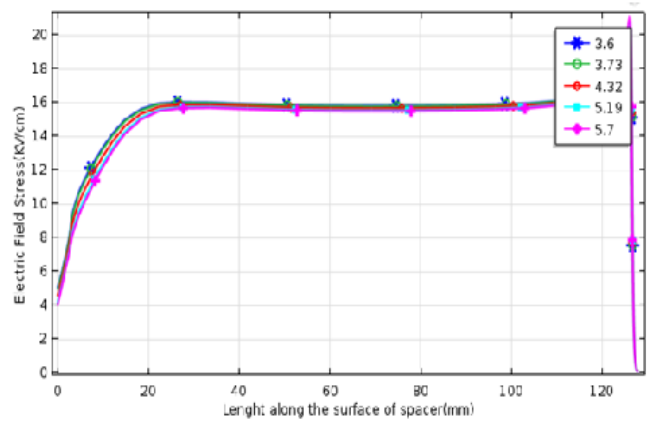


Fig. (b) With metal inserts

(ii) At 145KV voltage

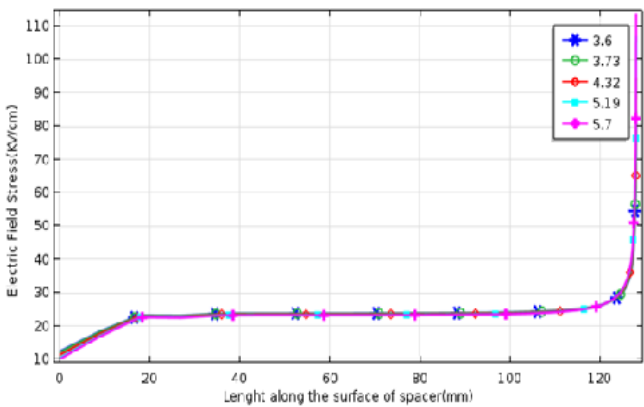


Fig. (a) Without metal inserts

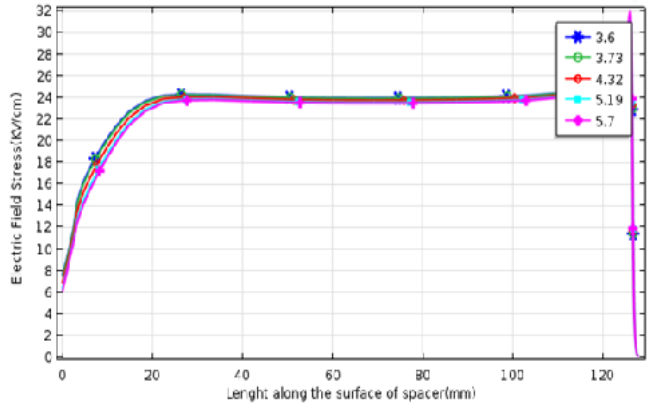


Fig. (b) With metal inserts

(iii) At 220KV voltage

Fig.5 Electric field stress with metal inserts under void for Titanium dioxide filler

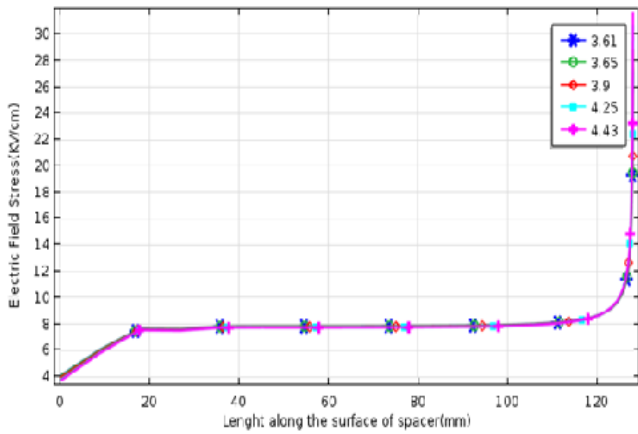


Fig. (a) Without metal inserts

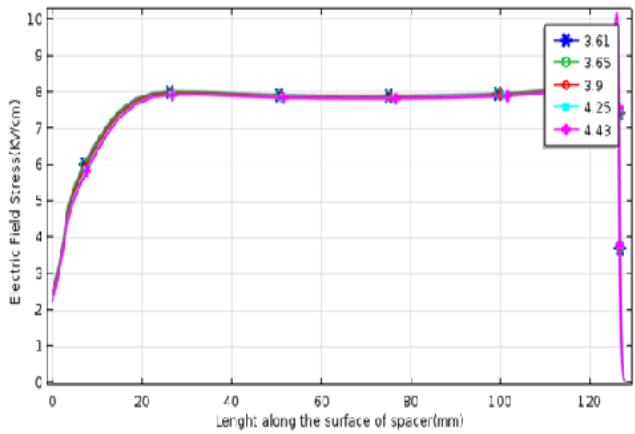


Fig. (b) With metal inserts

(i) At 72.5KV voltage

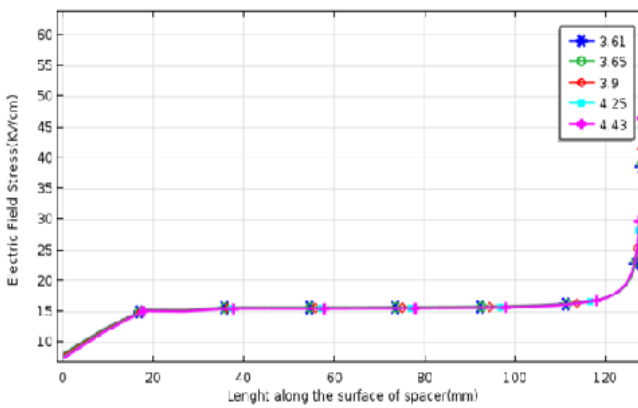


Fig. (a) Without metal inserts

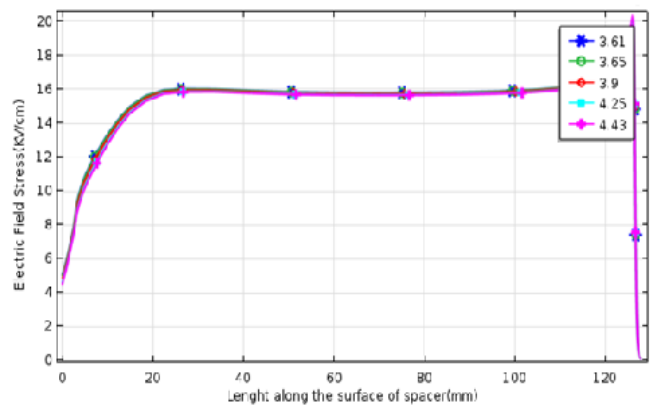


Fig. (b) With metal inserts

(ii) At 145KV voltage

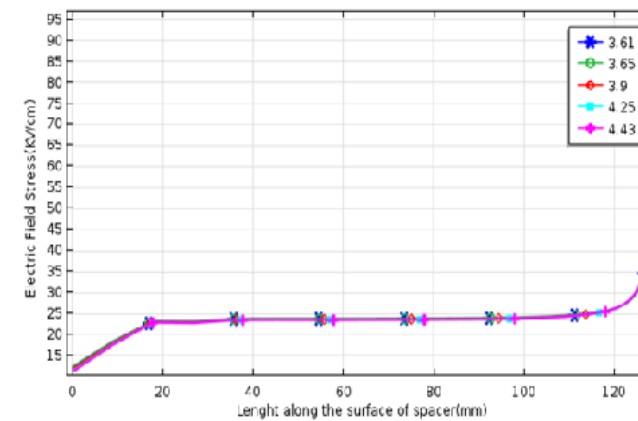


Fig. (a) Without metal inserts

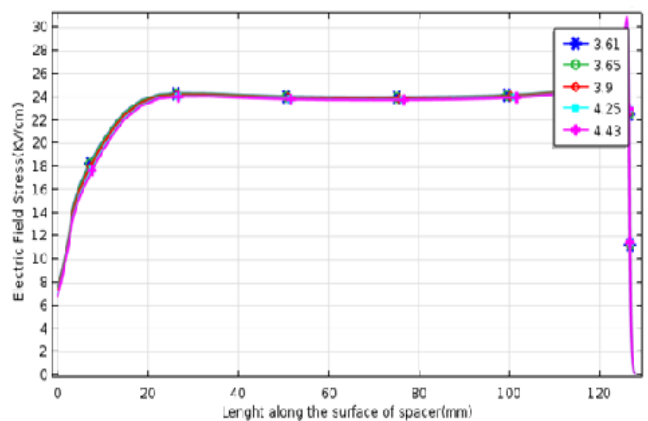


Fig. (b) With metal inserts

(iii) At 220KV voltage

Fig.6 Electric field stress with metal inserts under void for Magnesium oxide filler

Design and Analysis of Gas Insulated Busduct with Polymeric Spacers under Void defect

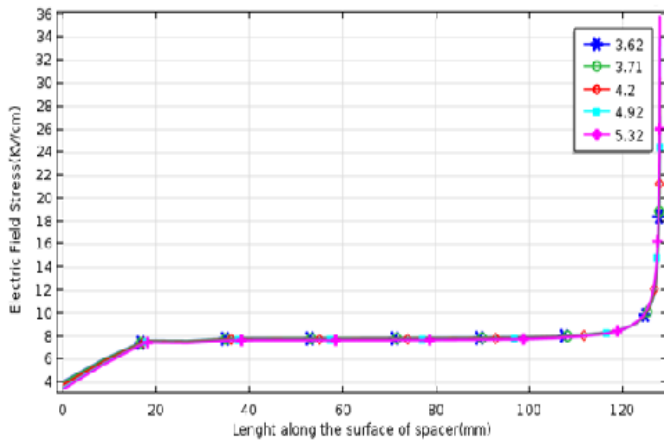


Fig. (a) Without metal inserts

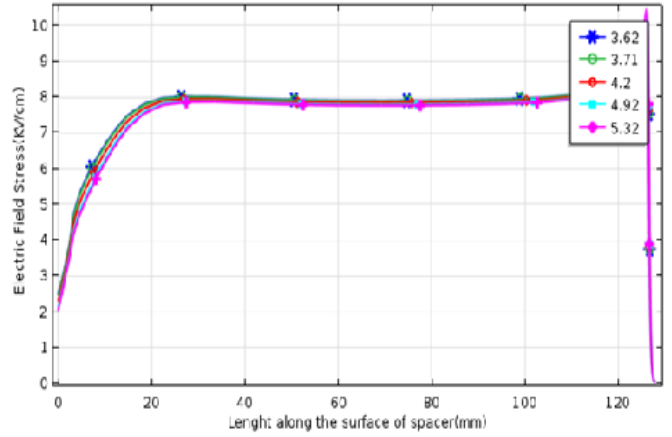


Fig. (b) With metal inserts

(i) At 72.5KV voltage

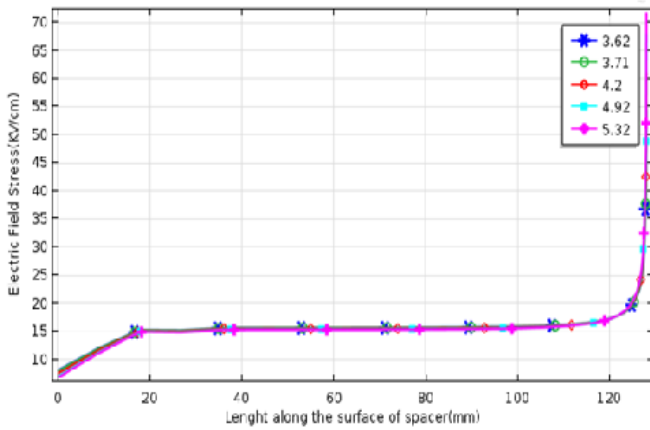


Fig. (a) Without metal inserts

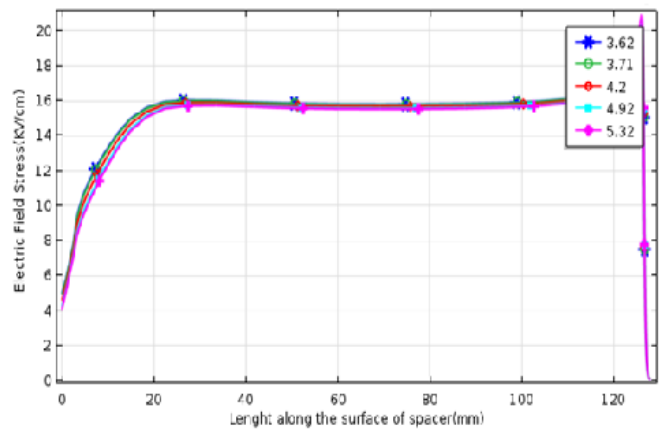


Fig. (b) With metal inserts

(ii) At 145KV voltage

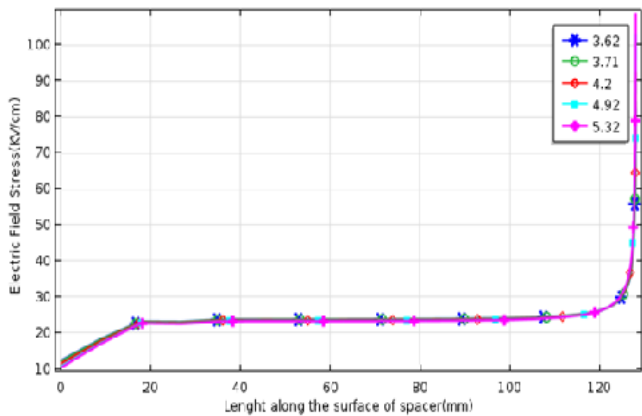


Fig. (a) Without metal inserts

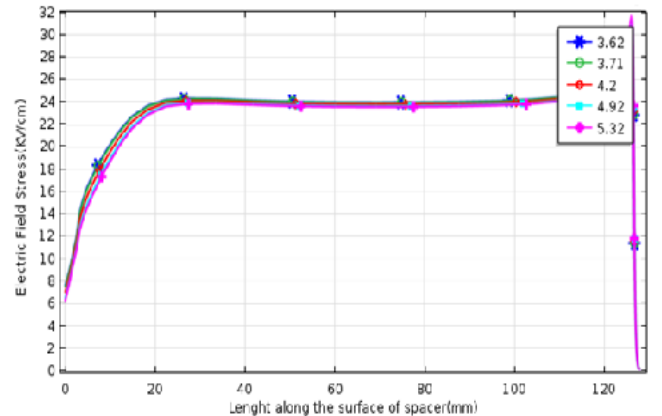


Fig. (b) With metal inserts

(iii) At 220KV voltage

Fig.7 Electric field stress with metal inserts under void for Boron carbide filler

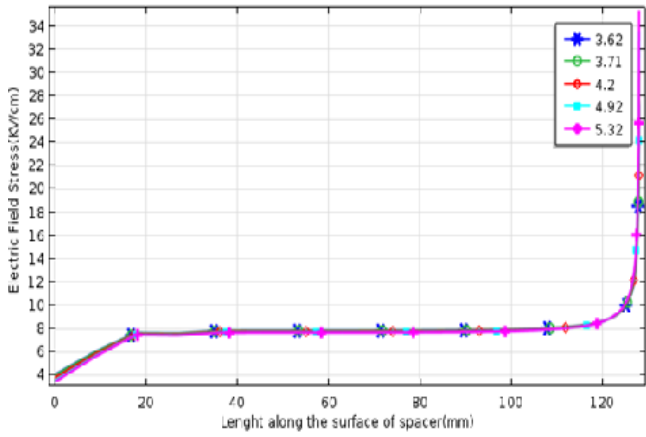


Fig. (a) Without metal inserts

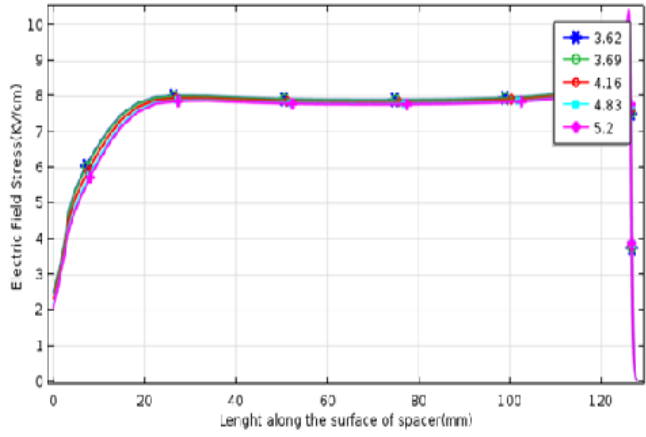


Fig. (b) With metal inserts

(i) At 72.5KV voltage

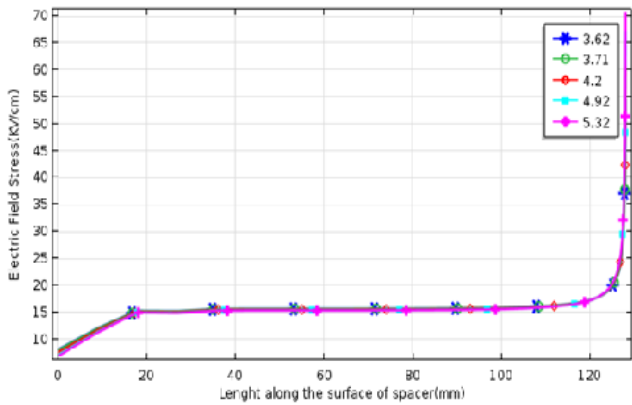


Fig. (a) Without metal inserts

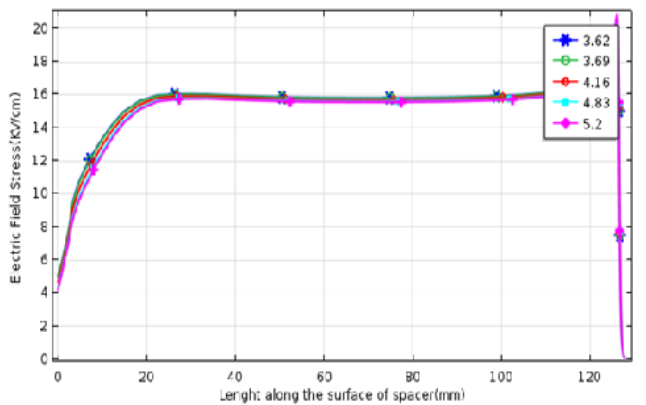


Fig. (b) With metal inserts

(ii) At 145KV voltage

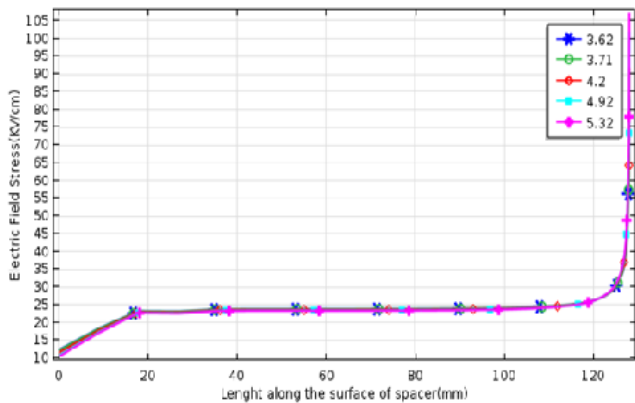


Fig. (a) Without metal inserts

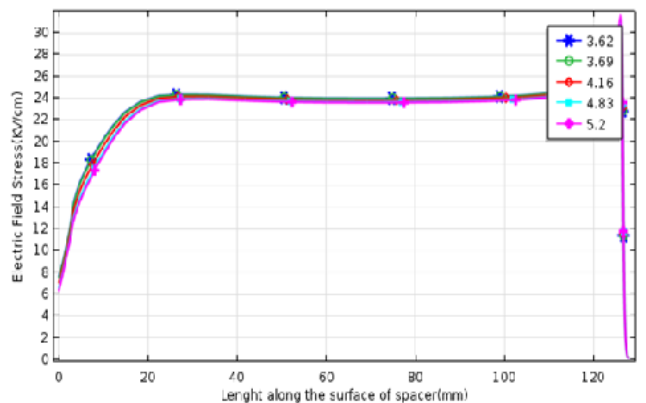


Fig. (b) With metal inserts

(iii) At 220KV voltage

Fig.8 Electric field stress with metal inserts under void for Silicon carbide filler

Design and Analysis of Gas Insulated Busduct with Polymeric Spacers under Void defect

Table 1: Electrical field stress for various voltages and different nitrate filler concentrations

Filler concentration	Resultant permittivity	72.5KV						145KV						220KV					
		Electric Field Stress Inner			Electric Field Stress Outer			Electric Field Stress Inner			Electric Field Stress Outer			Electric Field Stress Inner			Electric Field Stress Outer		
		plain-polymer	without MI	with MI	plain-polymer	without MI	with MI	plain-polymer	without MI	with MI	plain-polymer	without MI	with MI	plain-polymer	without MI	with MI	plain-polymer	without MI	with MI
0.2	3.61	3.89148	4.02715	2.49900	10.60880	27.1700	0.0592	7.783	8.0540	4.9990	21.2171	54.3700	0.1184	11.8086	12.220	7.5840	32.19	82.5080	0.1796
0.8	3.64	3.8794	4.01049	2.48700	10.61540	27.3600	0.0591	7.7588	8.0210	4.9740	21.231	54.7250	0.1183	11.772	12.170	7.5480	32.21	83.0350	0.1795
4	3.86	3.755	3.896	2.40500	10.68640	28.6132	0.0580	7.5095	7.7925	4.8100	21.373	57.2250	0.1175	11.394	11.823	7.2980	32.428	86.8050	0.1780
8	4.14	3.6149	3.768	2.31410	10.77000	30.1394	0.0580	7.23	7.5370	4.6282	21.54	60.2790	0.1165	10.9694	11.436	7.0220	32.68	91.4570	0.1768
10	4.3	3.543	3.703	2.26800	10.81470	30.9800	0.0579	7.086	7.4060	4.5360	21.6294	61.9605	0.1159	10.7511	11.238	6.8220	32.817	94.0090	0.1758

(a) Silica Nitrates

Filler concentration	Resultant permittivity	72.5KV						145KV						220KV					
		Electric Field Stress Inner			Electric Field Stress Outer			Electric Field Stress Inner			Electric Field Stress Outer			Electric Field Stress Inner			Electric Field Stress Outer		
		plain-polymer	without MI	with MI	plain-polymer	without MI	with MI	plain-polymer	without MI	with MI	plain-polymer	without MI	with MI	plain-polymer	without MI	with MI	plain-polymer	without MI	with MI
0.2	3.61	3.8915	4.027	2.49950	10.60880	27.1850	0.0592	7.783	8.0543	4.9990	21.2175	54.3800	0.1184	11.8086	12.220	7.5850	32.192	82.4850	0.1796
0.8	3.66	3.8675	3.999	2.47900	10.62220	27.4700	0.0591	7.735	7.9990	4.9590	21.2442	54.9500	0.1182	11.7358	12.137	7.5240	32.2328	83.3750	0.1794
4	3.94	3.7128	3.858	2.37750	10.71100	29.0567	0.0586	7.426	7.7159	4.7550	21.422	58.1132	0.1173	11.2666	11.707	7.2150	32.5026	88.1400	0.1779
8	4.32	3.5344	3.6955	2.26250	10.82000	31.0840	0.0579	7.069	7.3910	4.5250	21.64	62.1670	0.1158	10.725	11.214	6.8655	32.834	94.3230	0.1778
10	4.52	3.4522	3.6212	2.21050	10.87280	32.0990	0.0575	6.905	7.2420	4.4210	21.7455	64.2010	0.1150	10.476	10.988	6.7070	32.9935	97.4090	0.1745

(b) Aluminium Nitrates

Table 2: Electrical field stress for various voltages and different oxide filler concentrations

Filler concentration	Resultant permittivity	72.5KV						145KV						220KV					
		Electric Field Stress Inner			Electric Field Stress Outer			Electric Field Stress Inner			Electric Field Stress Outer			Electric Field Stress Inner			Electric Field Stress Outer		
		plain-polymer	without MI	with MI	plain-polymer	without MI	with MI	plain-polymer	without MI	with MI	plain-polymer	without MI	with MI	plain-polymer	without MI	with MI	plain-polymer	without MI	with MI
0.2	3.6	3.904	4.0328	2.504	10.60200	27.1280	0.0592	7.8073	8.0650	5.0072	21.204	54.2600	0.1183	11.8456	12.230	7.5970	32.1718	82.3270	0.1796
0.8	3.73	3.8267	3.962	2.4525	10.64500	27.8780	0.0590	7.6534	7.9242	4.9048	21.2902	55.7600	0.1180	11.612	12.023	7.4410	32.302	84.6030	0.1790
4	4.32	3.53438	3.6955	2.2625	10.82000	31.0790	0.0579	7.06874	7.3910	4.5250	21.64	62.1677	0.1159	10.725	11.214	6.8655	32.8335	94.3200	0.1759
8	5.19	3.2227	3.4146	2.068	11.02940	35.2700	0.0561	6.4454	6.8292	4.1360	22.058	70.5100	0.1121	9.779	10.361	6.2750	33.4681	107.0400	0.1702
10	5.7	3.0838	3.2905	1.984	11.13170	37.4700	0.0551	6.1676	6.5810	3.9680	22.2633	74.9350	0.1100	9.35774	9.985	6.0206	33.779	113.7000	0.1670

(a) Titanium dioxide

Filler concentration	Resultant permittivity	72.5KV						145KV						220KV					
		Electric Field Stress Inner			Electric Field Stress Outer			Electric Field Stress Inner			Electric Field Stress Outer			Electric Field Stress Inner			Electric Field Stress Outer		
		plain-polymer	without MI	with MI	plain-polymer	without MI	with MI	plain-polymer	without MI	with MI	plain-polymer	without MI	with MI	plain-polymer	without MI	with MI	plain-polymer	without MI	with MI
0.2	3.61	3.8975	4.027	2.50000	10.60540	27.1840	0.0592	7.7951	8.0540	5.0000	21.2108	54.3780	0.1184	11.827	12.220	7.5850	32.182	82.4960	0.1796
0.8	3.65	3.87343	4.005	2.48300	10.61880	27.4200	0.0590	7.74686	8.0100	4.9660	21.2375	54.8250	0.1183	11.7539	12.153	7.5360	32.2226	83.2070	0.1794
4	3.9	3.7336	3.877	2.39100	10.69880	28.8210	0.0587	7.4672	7.7538	4.7820	21.3978	57.6715	0.1174	11.33	11.764	7.2250	32.4655	87.5020	0.1781
8	4.25	3.5649	3.723	2.28200	10.80100	30.7150	0.0580	7.1298	7.4464	4.5640	21.6019	61.4400	0.1161	10.8176	11.298	6.9250	32.7753	93.2190	0.1761
10	4.43	3.48832	3.653	2.23300	10.84950	31.6400	0.0577	6.97662	7.3070	4.4665	21.6989	63.2900	0.1154	10.5851	11.087	6.7760	32.9225	96.0330	0.1750

(b) Magnesium Oxide

Table 3: Electrical field stress for various voltages and different Carbide filler concentrations

Filler concentration	Resultant permittivity	72.5KV						145KV						220KV					
		Electric Field Stress Inner			Electric Field Stress Outer			Electric Field Stress Inner			Electric Field Stress Outer			Electric Field Stress Inner			Electric Field Stress Outer		
		plain-polymer	without MI	with MI	plain-polymer	without MI	with MI	plain-polymer	without MI	with MI	plain-polymer	without MI	with MI	plain-polymer	without MI	with MI	plain-polymer	without MI	with MI
0.2	3.62	3.8915	4.0215	2.49550	10.60870	27.2400	0.0591	7.783	8.0430	8.0430	21.2175	54.4900	0.1184	11.8086	12.203	7.5720	32.192	82.6800	0.1792
0.8	3.71	3.8382	3.972	2.46000	10.63860	27.7600	0.0590	7.6764	7.9450	7.9450	21.277	55.5300	0.1183	11.647	12.055	7.4640	32.2827	84.2500	0.1790
4	4.2	3.587	3.7435	2.29600	10.78700	30.4500	0.0581	7.175	7.4870	7.4870	21.574	60.8090	0.1175	10.857	11.360	6.9680	32.733	92.4100	0.1760
8	4.92	3.3078	3.491	2.12000	10.96950	34.0370	0.0567	6.6156	6.9820	6.9820	21.939	68.0740	0.1161	10.0375	10.590	6.4340	32.286	103.2850	0.1720
10	5.32	3.1848	3.3806	2.04500	11.05670	35.8500	0.0559	6.3696	6.7610	6.7610	22.1135	71.7020	0.1150	9.665	10.259	6.2050	33.5515	108.7900	0.1690

(a) Boron Carbide



Filler concentration	Resultant permittivity	72.5KV						145KV						220KV					
		Electric Field Stress Inner			Electric Field Stress Outer			Electric Field Stress Inner			Electric Field Stress Outer			Electric Field Stress Inner			Electric Field Stress Outer		
		plain-polymer	without MI	with MI	plain-polymer	without MI	with MI	plain-polymer	without MI	with MI	plain-polymer	without MI	with MI	plain-polymer	without MI	with MI	plain-polymer	without MI	with MI
0.2	3.62	3.8915	4.0215	2.49550	10.60880	27.2400	0.0591	7.782	8.0430	4.9910	21.2176	54.4960	0.1184	11.8087	12.203	7.5720	32.192	82.6800	0.1793
0.8	3.69	3.8498	3.9833	2.46770	10.63200	27.6520	0.0590	7.699	7.9660	4.9355	21.264	55.3040	0.1181	11.682	12.087	7.4883	32.2628	83.9090	0.1790
4	4.16	3.6056	3.76	2.30800	10.77500	30.2450	0.0581	7.211	7.5200	4.6162	21.551	60.4920	0.1165	10.94	11.410	7.0040	32.6989	91.7800	0.1765
8	4.83	3.3382	3.518	2.13920	10.94880	33.6120	0.0567	6.6765	7.0366	4.2784	21.897	67.2250	0.1136	10.13	10.676	6.4910	33.224	101.9908	0.1722
10	5.2	3.2197	3.412	2.06600	11.03000	35.3190	0.0560	6.4395	6.8240	4.1325	22.06	70.6400	0.1123	9.77	10.353	6.2700	33.475	107.1750	0.1700

(b) Silicon Carbide

REFERENCES

- C.M. Cooke, A.H. Cookson, "The Nature and Practises of Gas as Electric Insulator", IEEE Transactions on Electrical Insulation, Volume: EI-13, Issue: 4, 1978, Page(s) 239 – 248.
- K.D. Srivastava and M.M. Morcos, "A Review of Some Critical Aspects of Insulation Design of GIS/GIL Systems", IEEE Transactions on Dielectrics and Electrical Insulation, pp.787-792, 2001.
- A.Arora, H.Koch, "Design Features of GIS:", IEEE Power Engineering Society General Meeting, 2005. Vol. 1, Publication Year : 2005, Page(s): 927 – 929.
- K. Polivanov, Theoretical Foundations of Electrical Engineering, part 3, Energiya, Moscow,1969.
- K. Nakanishi, A. Yoshioka, Y. Arahata, and Y. Shibuya, "Surface Charging on Epoxy Spacer at dc Stress in Compressed SF₆ Gas", IEEE Trans. Power Appar. Syst., Vol. PAS-102, pp. 3919-3927, 1983.
- F. Messerer and W. Boeck, "Field Optimization of an HVDC – GIS-Spacer", Annual Report, IEEE Conference Electric Insulation Dielectric Phenomena (C.E.I.D.P.), Atlanta, 1998, pp. 15 – 18.
- I.S.Han, J.K. Park, S.W.Min, E.S.Kim "Design of 170KV GIS Spacer By Using NURB Curve", International Conference on Electric Engineering, 2002.
- T.Takuma, T.Watanabe "Optimal Profiles Of Disc-Type Spacer For Gas Insulation", Proc. IEE, Vol. 122, No. 2, February 1975, pp. 183 – 188.
- Cronin, J.C.Perry, E.R: "Optimization of Insulators For Gas Insulated Systems", IEEE Trrans. Power Appar. Syst., 1973, PAS-92, (2), pp. 558 -564.
- Maren Istad, Magne Runde, Thirty-six years of service experience with a national population of gas-insulated substations, IEEE Trans. Power Delivery 25 (4) (2010).
- Alan H. Cookson, Review of high voltage gas breakdown and insulators in compressed gases, in: IEEE Proc. On Physical Science, Measurement and Instrumentation, Management and Education, 1981, pp. 303 – 312.
- H.Tsuboi, T. Misaki, Optimization of electrode and insulator contours by using Newton method, IEEE Trans. Japan, 106A (1986) 307 - 314.
- B. Weedy, "DC Conductivity of Voltalit Epoxy Spacers in SF₆", IEE Proc., Vol. 132, pt. A, pp. 450-454, 1985.
- V. Varivodav and E. Volpov, "Study of SF₆ /epoxy Insulation Properties at High Direct Stress", 6th Int. Symposium on High Voltage Engineering, (ISH), New Orleans, USA, paper 32.35, 1989.
- H. Fujinami, T. Takuma, and M. Yashima, "Mechanism and Effect of dc Charge Accumulation on SF₆ Gas Insulated Spacers", IEEE Trans. Power Delivery, Vol. 4, pp. 1765-1772, 1989.
- Huicheng Shi, Naikui Gao, Haiyun Jin, Gang Zhang, Zongren Peng " Investigation of the Effects of Nano-filler on Dielectric Properties of Epoxy Based Composites "; Proceedings of the 9th International Conf on Properties and Applications of Dielectric Materials July 19-23,2009, Harbin, China
- P. Preetha and M. Joy Thomas "AC Breakdown Characteristics of Epoxy Nanocomposites "IEEE Transactions on Dielectrics and Electrical Insulation Vol. 18, No. 5; October 2011.
- K.Y. Lau, M.A.M. Piah, " Polymer Nanocomposites in High Voltage Electrical Insulation Perspective: A Review", Malaysian Polymer Journal, Vol. 6, No. 1 , p 58 – 69, 2011.
- J.M.K. MacAlpine, M.A., PhD., A.Inst.P., and A.H. Cookson, B.Sc. (Eng.), PhD., A.Inst.P., C.Eng., M.I.E.E. "Impulse Breakdown of Compressed Gases between Dielectric – covered electrodes" Proc. IEE, Vol. 117, No. 3, March 1970.
- R. Kochetov, T. Andritsch, U. Lafont, P.H.F. Morshuis, S.J. Picken, J.J. Smit "Thermal Behaviour of Epoxy Resin Filled with High Thermal Conductivity Nanopowders" IEEE electrical Insulation Conference, Montreal, QC, Canada, 31 May – 3 June 2009.